Motion detection in helical CT using data consistency conditions

Mélanie Mouchet, Simon Rit, Jean Michel Létang

Motion detection in helical CT using data consistency conditions

Simon Rit, Mélanie Mouchet, Jean Létang

Motion detection in helical CT using data consistency conditions

Mélanie Mouchet, Simon Rit and Jean Michel Létang

***Abstract*—In computed tomography (CT), unexpected motion can result in poor image quality after reconstruction. One way to detect this motion is to verify data consistency conditions (DCC). DCC are mathematical relationships that characterize the redundancy of the data and must be verified by the projections. Necessary conditions for cone-beam projections with a linear source trajectory state that the integral of the cosine weighted projections along each row of the detector must be equal. In this work, we apply these conditions to pairs of source positions along a helical trajectory by rebinning the projections to a virtual detector parallel to the line connecting the two source positions. Then, we construct a graph connecting source positions between which we can calculate DCC and we use the Dijkstra algorithm to compute the shortest path between the first source position and all the other ones. This method was tested on simulated projections of the dynamic version of the Forbild thorax phantom, mostly static at end-inhale except for one breathing cycle during the acquisition. The proposed method allows a clear identification of when motion occurs during the acquisition.**

***Index Terms*—Computed tomography, data consistency conditions, motion detection**

I. Introduction

COMPUTED tomography (CT) assumes that the patient remains static during the acquisition. Breath-hold acquisitions, in particular, require that patients hold their breath at a given position of their respiratory cycle but they might not manage breath-hold for the entire acquisition, thus creating inconsistencies in the acquired projections and artefacts in reconstructed images.

One way to check for the presence of motion is to use Data Consistency Conditions (DCC). They are mathematical relationships that must be verified by the measured data [1]. If unexpected motion occurs, DCC will generally not be verified by the projections. DCC have proven able to detect motion and to calibrate the geometry of the scanner but have mostly been used with circular source trajectories [1] [2] [3].

The main goal of this work is the use of pairwise cone-beam DCC to detect unexpected motion in helical CT.

II. Methods

A. Cone-beam pairwise DCC

Let $\vec{s}_{\lambda_i}$ and $\vec{s}_{\lambda_j}$ be two source positions on a linear trajectory parallel to the detector plane. The distance between the X-ray sources and the detector plane is D and a detector pixel is defined by its coordinates (u, v) in the detector's frame, where the u axis is parallel to the linear trajectory of the source. For each row v_k of the detector, we define:

$$M_{j,k}(\lambda_i) = \frac{1}{\sqrt{v_k^2 + D^2}} \int_{\mathbb{R}} g(\lambda_i, u, v_k) \frac{\sqrt{v_k^2 + D^2}}{\sqrt{u^2 + v_k^2 + D^2}} \mathrm{d}u. \quad (1)$$

with $g(\lambda_i, ., v_k)$ the fan-beam projection at angle λ_i and detector height v_k. The cone-beam pairwise DCC proposed by Levine et al [4] states that for each row v_k, if the projections are not laterally truncated (in the u direction) and the trajectory and the object do not intersect, then

$$M_{j,k}(\lambda_i) = M_{i,k}(\lambda_j). \quad (2)$$

Those DCC are mathematically equivalent to the zero-order fan-beam DCC proposed by Clackdoyle [5]. Indeed, the weight inside the integral is exactly the cosine of the angle between a ray and the central ray of the fan in the plane defined by the two source positions and the detector line v_k.

B. Cone-beam pairwise DCC in helical CT

In diagnostic helical CT, the detector is cylindrical and is not parallel to the trajectory line defined by two source positions. As a result, a pre-processing step of the measured data is necessary to apply the DCC. For a pair of projections, one can rebin the projections into a virtual detector with rows parallel to the line connecting the two corresponding source positions, as illustrated in Fig. 1. Such a process has already been described for a circular trajectory and flat detectors [2], we simply adapted it to the helical trajectory with a cylindrical detector.

DCC for a pair of projections can only be computed if a number of conditions is satisfied. The first one, mentioned above, imposes that the scanned object and the line connecting the two source positions do not intersect. Here, we impose that the line connecting the two source positions and the field-of-view (FOV) does not intersect as we do not assume prior knowledge but that the scanned object fits in the FOV. The second condition is the overlapping of the resampled projections on the virtual detector. For a circular trajectory, resampled projections overlap for any pair of sources. For the helical trajectory, as the detector, the source and the scanned object are also moving axially, resampled projections do not overlap for most pairs of projections. In addition, projections are not laterally truncated but may be axially truncated. Therefore, the DCC can only be computed for a pair of projections if there

Manuscript received December 12, 2020. This work was supported partly by a grant from the French national association for technical research (ANRT).

Mélanie Mouchet is with Siemens Healthcare, Paris, France and Université de Lyon, CREATIS; CNRS UMR5220; Inserm U1044; INSA-Lyon; Université Lyon 1; Centre Léon Bérard, France.

Jean Michel Létang and Simon Rit are with Université de Lyon, CREATIS; CNRS UMR5220; Inserm U1044; INSA-Lyon; Université Lyon 1; Centre Léon Bérard, France.

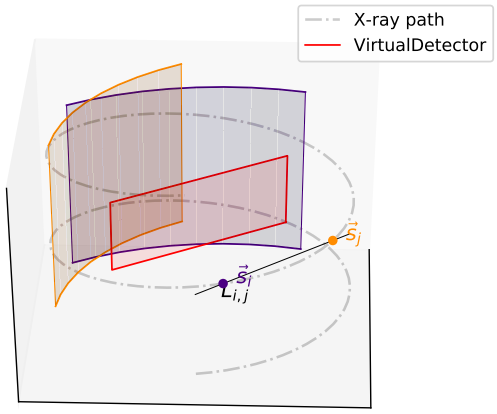

Fig. 1. Illustration of the rebinning of two projections for a helical trajectory. The virtual detector (red), is parallel to the line connecting the two source positions.

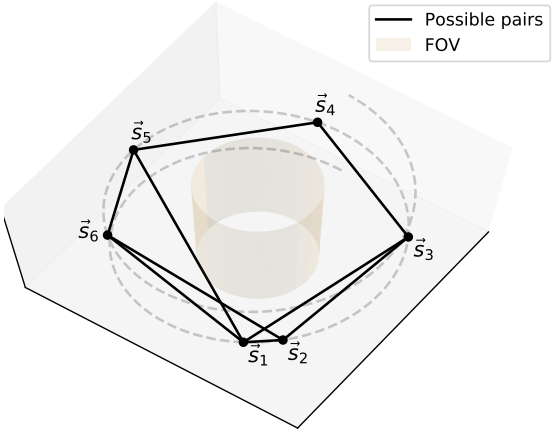

Fig. 2. Possible pairs computed for six source positions. The black lines illustrate pairs of source positions between which DCC can be computed. For example, one cannot compute a DCC between $\vec{s}_4$ and $\vec{s}_6$ but one can verify that $c_{4,5} + c_{5,6} = 0$.

is a plane that contains the two source positions and crosses the lateral borders of the two projections.

C. Motion detection in helical CT using a graph approach

These conditions prevent the computation of DCC between many pairs of projections but one can always connect two source positions with intermediate positions and verify that DCC are satisfied. To this end, we propose to construct a graph with the source positions as vertices and an edge between pairs fulfilling the conditions, weighted by the following cost $c_{i,j}$ to compare two cone-beam measurements $g(\lambda_i, ., .)$ and $g(\lambda_j, ., .)$:

$$c_{i,j} = \sqrt{\sum_{k=1}^{K} \frac{\left(M_{j,k}(\lambda_i) - M_{i,k}(\lambda_j)\right)^2}{K}} \tag{3}$$

where K is the number of rows of the virtual detector. If the data are consistent, then

$$c_{i,j} = 0 \tag{4}$$

and it is strictly positive otherwise. The graph is helpful to identify inconsistent projections. If two source positions i and j are directly connected, then the vertex cost $c_{i,j}$ is 0 if the projections are consistent, see Equation 4. In addition, if all projections are consistent along any path, then the sum of the vertex costs along the path is also zero.

To identify inconsistent projections, we therefore propose to use the shortest path between two source positions as a measure of the consistency between two source positions measured with Dijkstra's algorithm [6]. If the shortest path is not zero, there is no path between the two source positions with all projections consistent along the path.

D. Experiment

We simulated an acquisition of the 4D Forbild thorax phantom [7], Fig. 3, using the geometry of the Somatom Definition Flash Siemens CT scanner, with 100 projections per gantry rotation using the reconstruction toolkit (RTK [8]). Poisson noise was added to the projections. The number of photons received by a detector pixel after attenuation is between 10^2 and 10^7 in air. The acquisition takes 9 s and is divided in three parts. Between $t_0 = 0$ s and $t_1 = 3$ s, the phantom is static at end inhale. Between t_1 and $t_3 = 7$ s, the phantom breathes for one respiratory cycle, reaching end-exhale at $t_2 = 5.5$ s. It is back to its static position from end-inhale t_3 to $t_4 = 9.0$ s. Two reference projections are considered and the shortest path is computed with all the other source positions: t_0 and t_2.

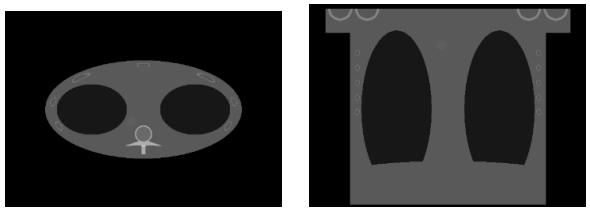

(a) Axial view of the phantom. (b) Coronal view of the phantom.

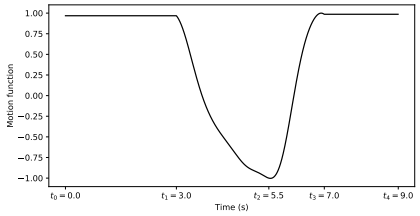

(c) Breathing signal of the phantom.

Fig. 3. Characteristics of the 4D Forbild thorax phantom.

III. Results

Fig. 4a shows the shortest path from the first projection t_0 at end-inhale to all the other ones. It is immediately possible to identify where motion occurs but we cannot identify that the phantom is back to end-inhale at t_3. This is because all paths pass by inconsistent intermediate positions between t_1 and t_3.

Fig. 4b shows the shortest path from the projection t_2, corresponding to end-exhale, to all the other ones. The pattern suggests a breathing period of $t_3 - t_1 = 4$ s since the inconsistency is constant from t_0 to t_1 and from t_3 to t_4. Fig. 4b strongly suggests that position $t_2 = 5.5$ s is inconsistent with all other projections.

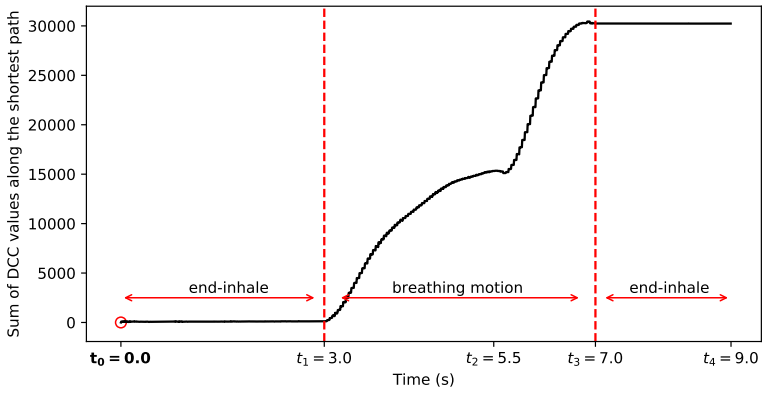

(a) Shortest path computed using reference time $t_0 = 0$ s.

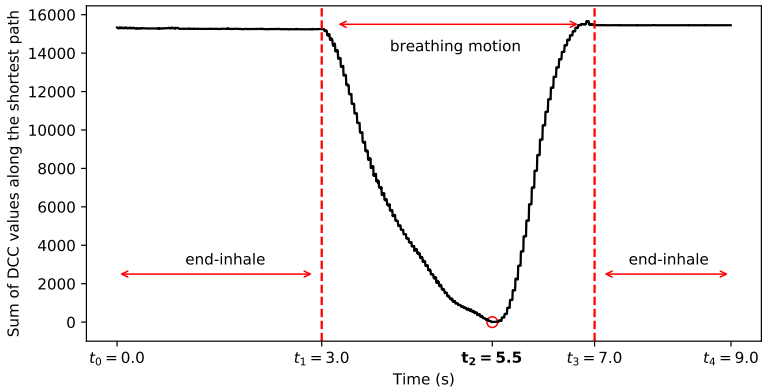

(b) Shortest path computed using reference time $t_2 = 5.5$ s.

Fig. 4. Shortest paths calculated from $t_0 = 0$ s (Fig. 4a) and $t_2 = 5.5$ s (Fig. 4b). The x-axis corresponds to the source positions. The y-axis corresponds to the sum of the cost $c_{i,j}$ (DCC measurement) along the shortest path with respect to the projection of reference (circled on the curve and in bold on the horizontal axis).

IV. Discussion and conclusions

We have proposed a graph approach to connect all source positions in helical CT using DCC.

Noise prevents the DCC to be exactly met but motion had a much stronger impact in this example. Cumulating the noise effect along the shortest path was deemed negligible compared to the level of inconsistency due to motion.

This proof-of-concept demonstrates the use of DCC in helical CT to detect motion during the acquisition. The graph approach is promising to select a group of consistent projections and, eventually, correct for motion artifacts in CT images.

References

[1] R. Clackdoyle, S. Rit, J. Hoskovec, and L. Desbat, "Fanbeam data consistency conditions for applications to motion detection," in *Third international conference on image formation in X-ray computed tomography*, 2014, p. 324–328.

[2] J. Lesaint, S. Rit, R. Clackdoyle, and L. Desbat, "Calibration for circular cone-beam CT based on consistency conditions," *IEEE Transactions on Radiation and Plasma Medical Sciences*, vol. 1, no. 6, pp. 517–526, 2017.

[3] A. Aichert, M. Berger, J. Wang, N. Maass, A. Doerfler, J. Hornegger, and A. K. Maier, "Epipolar consistency in transmission imaging," *IEEE Transactions on Medical Imaging*, vol. 34, no. 11, pp. 2205–2219, 2015.

[4] M. S. Levine, E. Y. Sidky, and X. Pan, "Consistency conditions for cone-beam CT data acquired with a straight-line source trajectory," *Tsinghua Science and Technology*, vol. 15, no. 1, pp. 56–61, 2010.

[5] R. Clackdoyle, "Necessary and sufficient consistency conditions for fan-beam projections along a line," *IEEE Transactions on Nuclear Science*, vol. 60, no. 3, pp. 1560–1569, 2013.

[6] E. Dijkstra, "A note on two problems in connexion with graphs." *Numerische Mathematik*, vol. 1, pp. 269–271, 1959.

[7] F. Bergner and M. Kachelrieß, "4D generalized thorax phantom," Institute of Medical Physics (IMP), Friedrich-Alexander-University of Erlangen-Nürnberg, Tech. Rep., 2009, http://www.imp.uni-erlangen.de/phantoms/thorax/4D_Thorax_Description.pdf.

[8] S. Rit, M. V. Oliva, S. Brousmiche, R. Labarbe, D. Sarrut, and G. C. Sharp, "The reconstruction toolkit (RTK), an open-source cone-beam CT reconstruction toolkit based on the insight toolkit (ITK)," *Journal of Physics: Conference Series*, vol. 489, p. 012079, mar 2014.